CARBON 49 (2011) 1568–1580

available at www.sciencedirect.com

ScienceDirect

journal homepage: www.elsevier.com/locate/carbon

Synthesis of high quality single-walled carbon nanotubes on natural sepiolite and their use for phenol absorption

*Jing-Qi Nie, Qiang Zhang, Meng-Qiang Zhao, Jia-Qi Huang, Qian Wen, Yu Cui, Wei-Zhong Qian *, Fei Wei*

Beijing Key Laboratory of Green Chemical Reaction Engineering and Technology, Department of Chemical Engineering, Tsinghua University, Beijing 100084, China

ARTICLE INFO

Article history:
Received 29 August 2010
Accepted 11 December 2010
Available online 16 December 2010

ABSTRACT

Natural sepiolite mineral was used as a catalyst and catalyst support for the efficient growth of single-walled carbon nanotubes (SWCNTs). With the introduction of hydrogen, uniform active metal nanoparticles can be formed in the fibrous structure of sepiolite ore. High-quality SWCNTs with few defects and a large aspect ratio (over 10^4) were synthesized. The structure of the CNTs was modified by controlling the catalyst composition with ion-exchange method and changing the growth conditions. The 1 wt.% Fe-based catalyst exhibited excellent activity for the growth of SWCNTs, while the Co/Mo-based catalyst preferred to grow small diameter SWCNTs. The reaction temperature showed a sensitive selectivity to the chirality and diameter distribution of the SWCNTs produced. Catalysts based on the sepiolite can also afford the effective growth of SWCNTs in a fluidized bed reactor. As-grown SWCNTs/calcined-sepiolite demonstrated excellent ability of phenol adsorption, with an adsorption capacity of 155.8 mg/g, which was much higher than that on natural sepiolite (12.7 mg/g).

1. Introduction

Single-walled carbon nanotubes (SWCNTs), as a novel quasi-one-dimensional material, have attracted tremendously attention because of their excellent properties. A wide range of applications, including composite materials, electrode materials for energy conversion and storage, nanoelectronics, and nano-scale sensors have been proposed [1–5]. The demand for high-quality SWCNTs is rising quickly. The efficient and controllable growth of SWCNTs is a prerequisite for their industrial application.

Many efforts have been made to find easy routes for the controllable growth of CNTs in a sustainable way. Growth of CNTs on natural materials is one of most potential ways to realize the environmentally benign and low-cost production [6]. Up to now, a series of minerals, such as volcanic lava rock [7,8], soil [6], garnet sand [9], wollastonites [10], bentonite [11], forsterite [12], diopside [12], montmorillonite [13,14], vermiculite [15–17], and biomass-based activated carbon [18–20], red mud (a toxic waste product from bauxite processing) [21] have been used as catalysts and/or catalyst supports for the synthesis of nanocarbon. The as-obtained products grown on natural materials have been used as catalysts in oxidative dehydrogenation (carbon nanofiber/lava [8] and CNT/bentonite [11]), functional materials for energy absorption (alternating aligned CNTs and vermiculite layers [15]), catalyst support, and fillers for strong polyamide-6 composites (CNT/clay hybrids) [14]. Producing CNTs on natural materials is a quite attractive method to obtain advanced functional materials for applications in material science and catalysis.

Nanocarbons synthesized on natural materials by far were mainly multi-walled CNTs (MWCNTs) and/or carbon

* *Corresponding author:* Fax: +86 10 6277 2051.
E-mail address: qianwz@mail.tsinghua.edu.cn (W.-Z. Qian).
0008-6223/$ - see front matter
doi:10.1016/j.carbon.2010.12.039

nanofibers with large diameters [6–11,13–20]. Few works on the efficient synthesis of SWCNTs were reported, which was mainly ascribed to the complex chemistry in the route for SWCNT growth [12]. The formation of small metal catalyst particles (0.5–5 nm) is the key factor for SWCNT production. However, metal particles dispersed on the minerals were prone to agglomerate into large particles, leading to the growth of MWCNTs. Thus, the chemical modulation for sustainable growth of SWCNTs on natural materials is still a great challenge.

Herein, the clay mineral sepiolite, which is a microcrystalline hydrated magnesium silicate of theoretical unit cell formula $Si_{12}O_{30}Mg_8(OH,F)_4(OH_2)_4{\cdot}8H_2O$, was used as catalyst or catalyst support for efficient growth of high-quality SWCNTs. The natural sepiolite exhibits a micro fibrous morphology. It has been widely used to fabricate various advanced functional materials, including functionalized carbon–silicates, micro fibrous chitosan-sepiolite nanocomposites [22], titania-sepiolite nanocomposites [23], hybrid materials formed by sequestration of pyridine molecules in the tunnels of sepiolite [24], graphene-like/sepiolite [25], and carbon nanofibers [26]. With a large surface area, regular pore structure, and fibrous morphology, the sepiolite was a good support for metal dispersion and can improve the thermal stability of nano-particles at high reaction temperature. The Fe element distributed in the sepiolite was the potential active catalyst source for CNT growth. However, the Fe content, usually less than 0.5 wt.% in the natural sepiolite, was too small to synthesize CNTs efficiently. Luckily, attributed to its high ion-exchange capacity, the active phase content (such as Fe, Co) can be easily increased by ion-exchange method, which provided enough active phase for the efficient growth of SWCNTs. Based on those consideration, we designed an easy but effective chemical route for SWCNT synthesis on unpurified sepiolite ore (Fig. 1). The natural sepiolite is composed of blocks similar to the layered clay minerals. Each block is formed by two tetrahedral silica sheets and a central octahedral sheet containing Mg^{2+} cations (Fig. 1a). The periodic inversion of silica tetrahedron creates abundant nano-scale channels and the Mg^{2+}, Ca^{2+} and K^+ cations were easily replaced by other metallic ions, such as Fe^{2+}, Fe^{3+}, or Co^{2+} (Fig. 1b). After the ion exchange, the sepiolite was dried and reduced, and small metal nanoparticles were formed on the sepiolite. With the introduction of CH_4 as carbon source during the chemical vapor deposition (CVD), SWCNTs would grow out. And structure and quality of SWCNTs were controlled by varying the key parameters, such as active metal species, loading amount, and growth temperature, in the mentioned route above. Meanwhile, the SWCNTs based on the sepiolite can be efficiently synthesized in both a fixed bed and a fluidized bed reactor. The as-obtained products from the sepiolite ore were used to adsorb phenol in water to explore its application in environmental protection.

2. Experimental

2.1. Catalyst preparation

The sepiolite used in our experiment was mined in Nanyang, Henan Province of China. In brief, the catalyst was prepared by ion-exchange method in which sepiolite powder with a size ranging from 10 to 300 μm was suspended in deionized water, and then a solution of $Fe(NO_3)_3{\cdot}9H_2O$ (or $Co(NO_3)_2{\cdot}6H_2O$ and $(NH_4)_6Mo_7O_{24}{\cdot}4H_2O$) was added slowly into the suspension under stirring. In order to enhance active metal iron exchange and dispersion, a 15 min ultrasonic treatment was performed, followed by drying at 100 °C for 24 h. Besides, the natural sepiolite ore was also used as the catalyst without any pre-treatment.

2.2. SWCNT synthesis in a fixed bed reactor

In the CVD growth, about 0.1 g catalyst was loaded into a horizontal quartz tube (30 mm id) and then heated in the flow of Ar (600 mL/min). Once the temperature of the furnace reached the growth temperature, such as 900 °C, a mixture of $CH_4/H_2/Ar$ (100, 10, and 400 mL/min, respectively) was introduced into the reactor for 15–30 min. Next, the products were cooled to ambient temperature under Ar protection and prepared for further characterization.

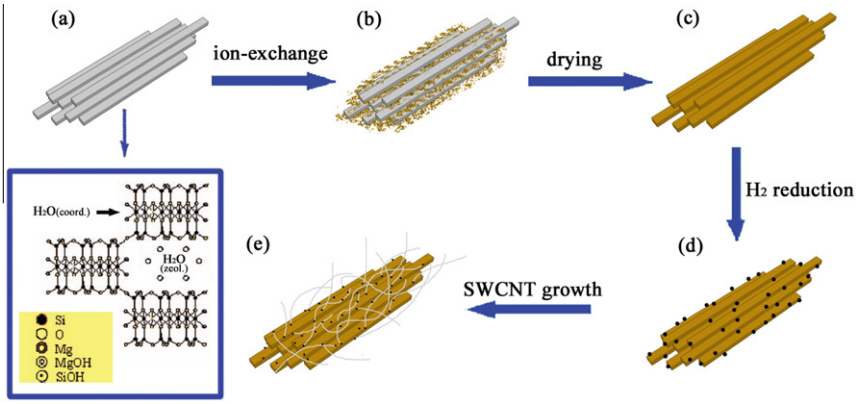

Fig. 1 – Illustration of the synthesis of SWCNTs. (a) The pristine structure of sepiolite. (b) The Fe^{3+} can exchange with Mg^{2+}, Ca^{2+} in the chain structure of sepiolite. After (c) drying and (d) reduction by H_2, Fe particles formed on the surface of fibrous structure or inside the tunnels. With introduction of CH_4, (e) SWCNTs efficiently grew on the sepiolite.

2.3. SWCNT synthesis in a fluidized bed reactor

In addition, the growth of SWCNTs on sepiolite catalyst was also carried out in a fluidized bed reactor similar to the previous studies [17]. The main quartz body was 1300 mm high and 50 mm in inner diameter with a sintered porous plate at the bottom to support the solid catalyst before fluidization and distribute the gas during the reaction. Here, about 1.0 g metal/sepiolite catalyst was loaded into the reactor and heated to 900 °C in the Ar flow (800 mL/min). The gas introduced at a sufficient velocity, through the bottom distributor, dispersed the catalyst particles and fluidized them smoothly. After that, the carbon source/H_2/Ar (600, 60, 100 mL/min, respectively) was fed into the fluidized bed to realize the synthesis of SWCNTs for 30 min, followed by cooling the furnace down at Ar atmosphere. The carbon product was then collected and characterized.

2.4. Phenol adsorption with SWCNT/cal-sepiolite com- posite

Phenol adsorption experiments were conducted with SWCNT/cal-sepiolite composite using a batch adsorption approach similar to that of Chen et al. [27]. Adsorption experiments were carried out in a 100-mL glass-stoppered flask. Approximate 0.1 g as-grown SWCNT product and natural sepiolite were put into the flask with 50 mL diluted phenol aqueous solution of the concentration ranged from 10 to 300 mg/L, respectively. And then, the flask was kept in a constant-temperature shaker bath at 30 °C, 100 rpm for 2 days to reach apparent sorption equilibrium (that was no further mass uptake) and the samples were centrifuged at 14,000 rpm for 20 min. To settle down the CNTs, another 24 h was taken to leave the samples undisturbed on a flat surface.

2.5. Characterization

The morphologies of the catalyst and SWCNT/cal-sepiolite samples were characterized using a JSM 7401F scanning electron microscope (SEM) operated at 3.0 kV, and a JEM 2010 high-resolution transmission electron microscope (TEM) operated at 120.0 kV. The samples for TEM observation were prepared through a common sonication method. To understand the structure of the catalyst better, X-ray fluorescence (XRF) was recorded on an XRF-1800. X-ray diffraction (XRD) pattern of the catalyst was recorded on a Rigaku D/max-RB diffractometer at 40.0 kV and 120 mA with Cu Kα radiation. The weight loss was obtained by thermogravimetry analysis (TGA), in which the sample was heated to 1200 °C at a rate of 10 °C/min using TGA Q500. The Brunauer-Emmett-Teller (BET) specific surface area was also measured by N_2 adsorption at liquid-N_2 low temperature using Micromeritics Flow Sorb II 2300. Besides, resonant Raman spectra of as-synthesized SWCNTs were obtained with lasers excitation at 514 and 633 nm using Renishaw RM2000 and at 532 nm using Horiba JY XploRA. UV–vis spectrophotometer (Shanghai Spectrum, Model SP-756PC) was used to analyze the concentrations of phenol at maximum ultraviolet adsorption wavelengths 269 nm.

3. Results and discussion

3.1. Catalyst derived from natural sepiolite for SWCNT growth

Natural sepiolite mineral powder was directly used as a catalyst and catalyst support without any further purification. It was noticed that the sepiolite mineral powder was in an agglomerated state with a diameter ranging from 5 to 300 μm (Fig. 2a). The SEM image (Fig. 2b) showed the fibrous microstructure. Furthermore, the compositions were determined by XRF analysis. As shown in Table 1, the natural sepiolite mineral itself contained a small amount of iron impurity except the major component 43.85 wt.% SiO_2, 26.13 wt.% CaO and 25.38 wt.% MgO. But ca. 0.36 wt.% Fe (0.51 wt.% Fe_2O_3) loading was low for the efficient fabrication of SWCNTs. The loading amount of active phase was increased by ion-exchange, as described in the experimental section.

Typical XRD pattern of the sepiolite sample at ambient temperature was given in Fig. 2c. The peaks in the pattern suggested that the mineral powder was a mixture of different compounds. The diffraction peaks of (1 1 0), (0 6 0), (2 6 0), (0 8 0), (3 7 1) crystal face of the sepiolite occurred up to 35° (2θ) [28], and the other peaks were assigned to zeolite ULM-5, Talc-2 M, syn-calcite and dolomite, respectively. The BET surface area of the sepiolite sample was only 31.5 m^2/g and TGA curves of the natural sepiolite were illustrated in Fig. 2d. The structure of sepiolite changed in two stages during the heating in nitrogen atmosphere: (i) the weight loss below 400 °C was attributed to the desorption of zeolitic water; (ii) the weight loss above 600 °C was due to the removal of coordinated water.

Ion-exchange in $Fe(NO_3)_3{\cdot}9H_2O$ solution was used to increase the metal active phase amount in the sepiolite, which would not destroy the fibrous structure (Fig. 2e) after drying in air atmosphere. The composition of the precursor with 1 wt.% Fe loading was recorded in Table 1. The change of composition proportion reveals that the Mg^{2+}, Ca^{2+} cations in the chain structure were partially replaced by Fe^{3+} iron, which was favorable for uniform distribution of the catalytic metal. As a result, the total iron content reached 1.73 wt.% (2.47 wt.% Fe_2O_3), almost three times of that in natural sepiolite, while other components were roughly with the same proportion. The Fe catalyst particles formed on the surface of fibrous structure if the Fe/sepiolite catalyst was reduced in H_2 condition at 900 °C. The blocks in structure weakened the sintering and resulted in the formation of nano-sized catalytic particles. As shown in TEM image (Fig. 2f), the black dots, indicating the active catalyst particles, distributed uniformly on the surface of the sepiolite fibers. This provided active sites for the synthesis of SWCNTs on the Fe/sepiolte catalyst.

3.2. Typical as-grown SWCNTs on the sepiolite

The SWCNTs grew from the active sites on the 1 wt.% Fe/sepiolite catalyst after the introduction of CH_4 into the reactor at a temperature of 900 °C. Similar to the products on other man-made supports, such as MgO [29], MCM-41 [30], zeolite [31] and FSM-16 [32], SWCNTs were in small bundles entangled with each other with a length of several-hundred microns

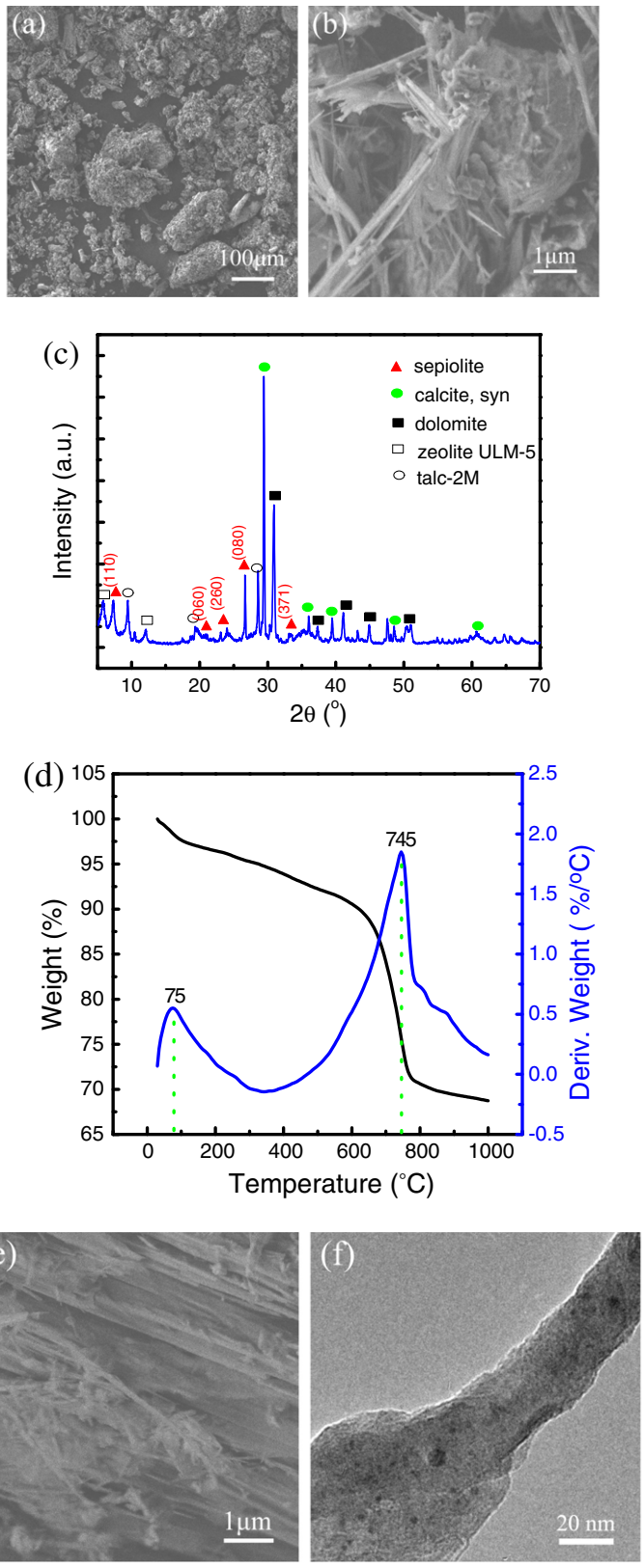

Fig. 2 – SEM images of the sepiolite sample: (a) a whole scene, (b) local microfiber structure. (c) The XRD pattern of natural sepiolite mineral powder. (d) TGA pattern of the sepiolite. (e) The fibrous structure of 1 wt.% Fe/sepiolite catalyst. (f) TEM image of Fe particles on the surface of fibrous structure.

(Fig. 3a). In addition, it was noticed that these bundles usually extended along the sepiolite fibers (Fig. 3a and b), not on the surface of other bulk impurities. The products were also well characterized by TEM. As illustrated in Fig. 3c, the SWCNTs

Table 1 – Composition of the natural sepiolite and 1 wt.% Fe/sepiolite catalyst determined by XRF.

Component	Sepiolite (wt.%)	1 wt.% Fe/sepiolite catalyst (wt.%)
SiO_2	43.85	43.75
CaO	26.13	25.87
MgO	25.38	24.25
Al_2O_3	3.45	3.04
Fe_2O_3	0.51	2.47
TiO_2	0.26	0.22
K_2O	0.21	0.20
P_2O_5	0.09	0.08
Cr_2O_3	0.05	0.05
Other	0.07	0.07

showed a clear single graphene layer with few defects. Meanwhile, the diameter distribution of SWCNTs was also given in Fig. 3d. It can be found that more than 90% of the products were SWCNTs and the diameters ranged from 0.8 to 3.2 nm. To further understand the SWCNT evolution, the initial growth of SWCNTs on the sepiolite was detected by limiting the growth time to 30 s (Fig. 3e). In reductive atmosphere, the Fe nanoparticles with diameters of 1–3 nm were formed directly by the structural Fe ions and dispersed on the surface of the sepiolite fibers. If the operation window was not appropriate, such as excessive supply of H_2 or carbon source, the Fe particles would sinter into iron clusters or large aggregates. The large Fe particles were unfavorable for the growth of SWCNTs and were easily deactivated by the surrounding graphene layers. As shown in Fig. 3f, the diameter of iron cluster was about 20 nm and it was wrapped by two graphene layers.

Raman spectra were employed to analyze the diameter distribution and the graphitization degree of the SWCNTs through three main signals: G band, D band, and radial breathing mode (RBM). The intensity ratios of D-band to G-band were 0.07, 0.14, and 0.08 when the excitation wavelength was 633, 514, and 532 nm, respectively (Fig. 4a–c). This indicated the high graphitization degree of the as-grown SWCNTs. Besides, sharp RBM peaks were also observed in different Raman spectra. The diameter distribution of SWCNT products can be estimated based on the following equation: $\omega = 248/d$ [33]. The strong peak ranges appeared on the RBM patterns at the three wavelengths 633, 514, and 532 nm corresponded to the diameter ranges of 1.0–1.9, 1.3–1.8, and 0.8–1.9 nm, respectively.

3.3. *Catalyst-dependent growth of SWCNTs on the sepiolite*

The structure of the CNTs synthesized on the sepiolite mineral can be effectively modulated by changing the amount of metal loading and the metal compositions. As shown in Table 2, the Fe-based catalysts with the mass percentage of Fe ranging from 0 to 10 wt.% were denoted as catalysts A–D, especially catalyst A was the sepiolite ores without any pretreatment, while 1 wt.%, 5 wt.% Co/Mo-based catalyst with the ratio of Co to Mo of 10:1 and 5 wt.% Co/Mo-based catalyst (Co:Mo = 3:1) were denoted as catalysts E–G. Due to the existence of Fe compounds in the natural sepiolite ores, SWCNTs can be obtained even on the sepiolite sample without any treatment followed by the introduction of CH_4 at 900 °C. However, the catalytic active sites were quite limited that the bundles of SWCNTs were rarely observed by the SEM. Through the TEM images, it was noticed that the sepiolite fiber was usually encapsulated by the graphene layers and there were some SWCNTs with the diameters of ca. 0.8 nm on the sepiolite (Fig. 5a). The intensity ratio of the D to G band was as high as 0.93 (Table 2). When the loading amount increased to 1 wt.% (catalyst B), more than 90% of the CNT products were SWCNTs. The value of I_D/I_G reduced to 0.07, and the distribution in diameter was estimated to be 0.8–1.9 nm based on the RBM peaks (Table 2). Yet, the TEM images recorded the diameter with a wide range from 0.8 to 3.2 nm (Fig. 5b). With the further increase of the loading amount, the percentage of SWCNTs decreased (Fig. 5e). Meanwhile, double-walled CNTs (DWCNTs), triple-walled CNTs (TWCNTs), even MWCNTs appeared (Fig. 5c and d). The changes of the diameter distribution and the wall number of CNTs were ascribed to the larger iron particles formed due to the high loading amount, similar to previous reports [34–36].

Compared with the Fe-based catalyst family, the Co/Mo-based catalyst showed higher selectivity to the SWCNTs with small diameters, similar to other reports [37,38]. The SEM image (Fig. 6a) of the products obtained on catalyst E demonstrated that the CNT bundles were obtained on the massive sepiolite fibers. But the density of bundles was lower than that on catalyst B. The high resolution TEM image (Fig. 6b) revealed that the as-grown CNTs on catalyst E were mainly SWCNT bundles, with some defects that caused the increase of I_D/I_G ratio to 0.23 (Table 2). However, the diameter distribution, ranging from 0.8 to 2.0 nm, was much narrower than that of the products grown on Fe-based catalyst with the similar metal loading amount. The downward trend in diameter was maintained even if the Co/Mo (10:1) loading amount was increased to 5 wt.% (Fig. 6c). As illustrated in Fig. 6d, the percentage of SWCNTs with the diameter smaller than 2 nm rose to 86%; and this was higher than that in the SWCNTs on Fe-based catalyst C (67%). Even when maintaining the Co/Mo loading amount at 5 wt.%, great changes in the diameter and wall number distributions can be observed when the ratio of Co to Mo became 3:1. Most of the products were large bundles of MWCNTs, as shown in Fig. 6e and f. Therefore, both the Fe and Co can be loaded on the natural sepiolite ores for the controllable growth of SWCNTs.

3.4. *Temperature-dependent growth of SWCNTs on the sepiolite*

In CVD growth, the temperature played a critical role in the formation of nano-sized active metal particles, which affected the structure of SWCNTs, such as the diameters and charities [16,39,40]. The growth of SWCNTs on the natural sepiolite mineral at various reaction temperatures with catalyst B using CH_4 as carbon source was conducted. The as-grown products were shown in Figs. 3 and 7.

At the temperature below 750 °C, nearly no SWCNTs can be synthesized due to the low activity of metal particle for CH_4 cracking. The morphologies of the sepiolite fibers were

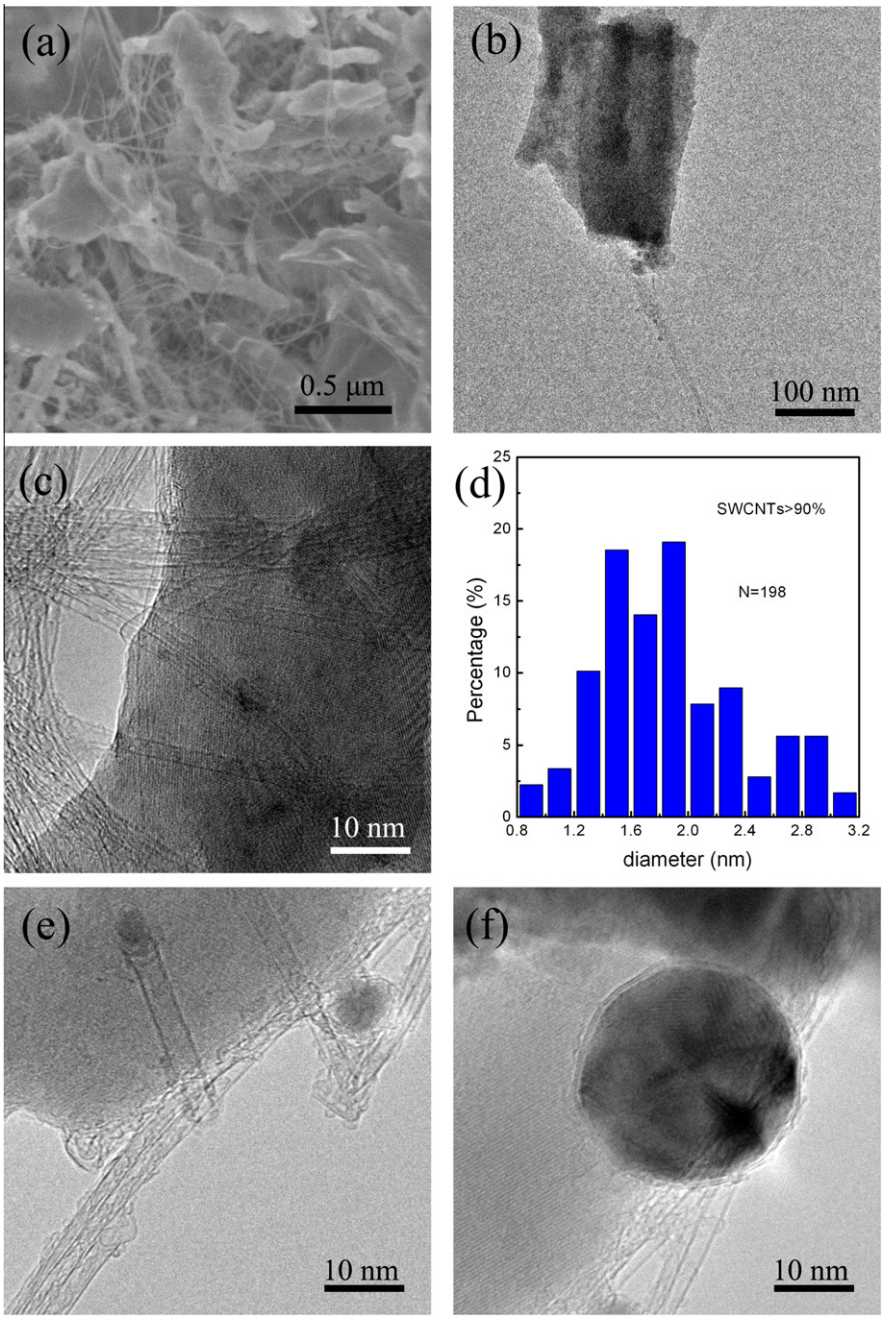

Fig. 3 – (a) The morphology of the SWCNTs formed on 1 wt.% Fe/sepiolite catalyst with CH_4 as carbon source at 900 °C. (b) Low magnification TEM image of CNT bundles among sepiolite microfiber structure. (c and d) High resolution TEM image and the diameter distribution of the SWCNT sample. (e and f) Initial growth of SWCNTs on the iron particles of the catalyst.

well preserved, but a few Fe particles formed and some amorphous carbon deposited on the surface of the support (Fig. 7a). When the reaction temperature was over 800 °C, SWCNTs were synthesized (Fig. 7b). The diameters of the SWCNTs ranged from 1.0 to 2.0 nm with the growth temperature of 800 °C. When the temperature increased to 850 °C, few SWCNTs with small diameter (<1.0 nm) were observed, and most of SWCNTs were with large diameters (>2.0 nm) in the products (Fig. 7c). The percentage of large diameter SWCNTs would further increase if growth temperature further increased (Fig. 7d). This was attributed to the severe metal sintering among the catalyst under higher temperature, which caused the formation of metal particles with larger diameters.

The Raman spectra, with the exciting wavelength of 633 and 514 nm, were recorded to characterize the structure and quality of the CNTs. In all, the I_D/I_G values at 800, 850, and 900 °C were low (Fig. 7e), indicating that the SWCNTs were all of high graphitization degree. The RBM peaks of the SWCNTs grown at different temperatures were illustrated in Fig. 7f. Moreover, the chirality of as-grown SWCNTs can be determined by the Kataura plot [41]. For the Raman spectra at 514 nm, it was found that the typical RBM region for

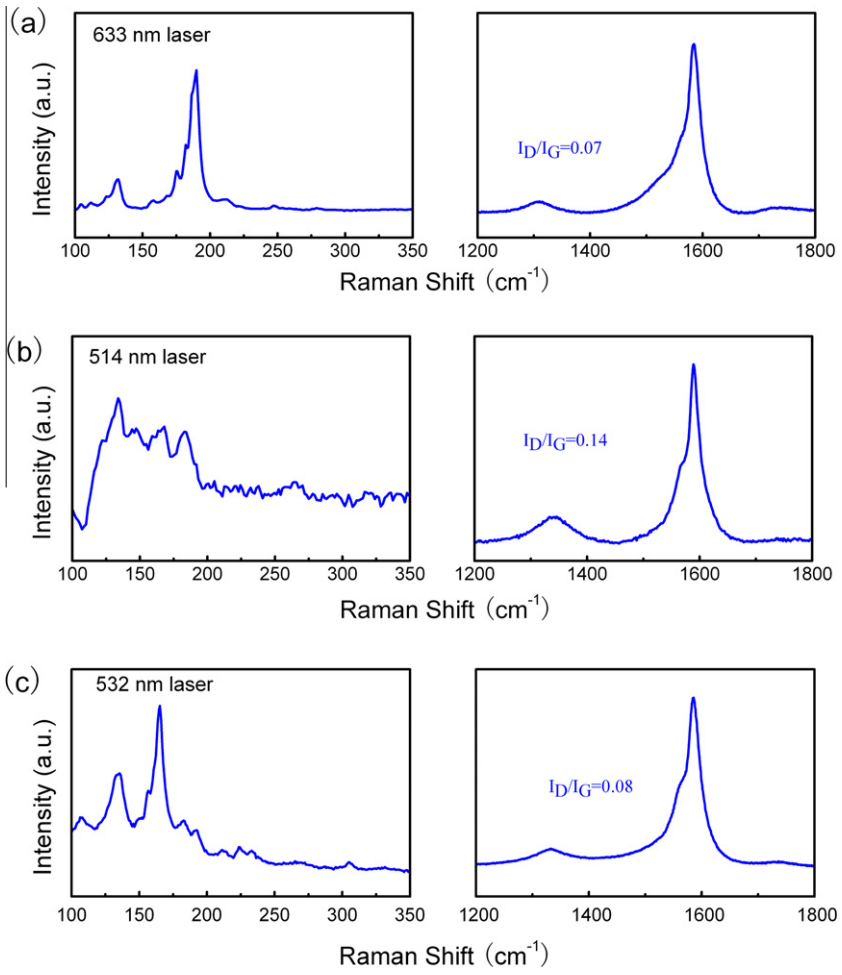

Fig. 4 – Raman spectra at excitation wavelength (a) 633, (b) 514, and (c) 532 nm for the SWCNT product on the 1 wt.% Fe/sepiolite catalyst at 900 °C.

Table 2 – Comparison of products on sepiolite minerals grown at 900 °C for 15 min.

Catalyst	Metal loading	Type[a]	I_D/I_G[b]	Diameter/nm[c]
A	None	SWCNTs/amorphous carbon	0.93	–
B	1 wt.% Fe	SWCNTs	0.07	0.8–3.2
C	5 wt.% Fe	S/FWCNTs	0.16	0.9–10
D	10 wt.% Fe	MWCNTs	0.21	3.0–30
E	1 wt.% Co/Mo(10:1)	SWCNTs	0.23	0.8–2.0
F	5 wt.% Co/Mo(10:1)	S/DWCNTs	0.12	0.8–2.6
G	5 wt.% Co/Mo(3:1)	MWCNTs/amorphous carbon	0.43	5.0–40

[a] The date was based on the statistical results by TEM images.
[b] The I_D/I_G ratio was obtained from the Raman spectra at excitation wavelength 633 nm.
[c] The diameter distribution was measured by TEM images.

semiconducting nanotubes, 126–186 cm^{-1}, was obvious when the reaction temperature was 850 °C. In contrast, the intensity of these peaks decreased significantly when the temperature was down to 800 °C and they nearly disappeared when the growth temperature was 900 °C. Besides, the peaks for metallic nanotubes at around 223 and 263 cm^{-1} were all weak. When the same products were excited by the 633 nm wavelength laser, there were mainly two strong peaks at around 132 and 190 cm^{-1}, corresponded to semiconducting and metallic nanotubes, respectively. However, according to the integral intensities of the relative peaks, the ratios of metallic to semi-conductive bands were variant, estimated to be about 9:1, 4:1 and 6:1 for 900, 850, and 800 °C, respectively.

3.5. *Growth of SWCNTs on the sepiolite in a fluidized bed reactor*

The intrinsic density of the natural sepiolite mineral was *ca.* 1000 kg/m^3 and the bulk density of the CNTs/cal-sepiolite agglomerates obtained in the fixed bed reactor was 530 kg/

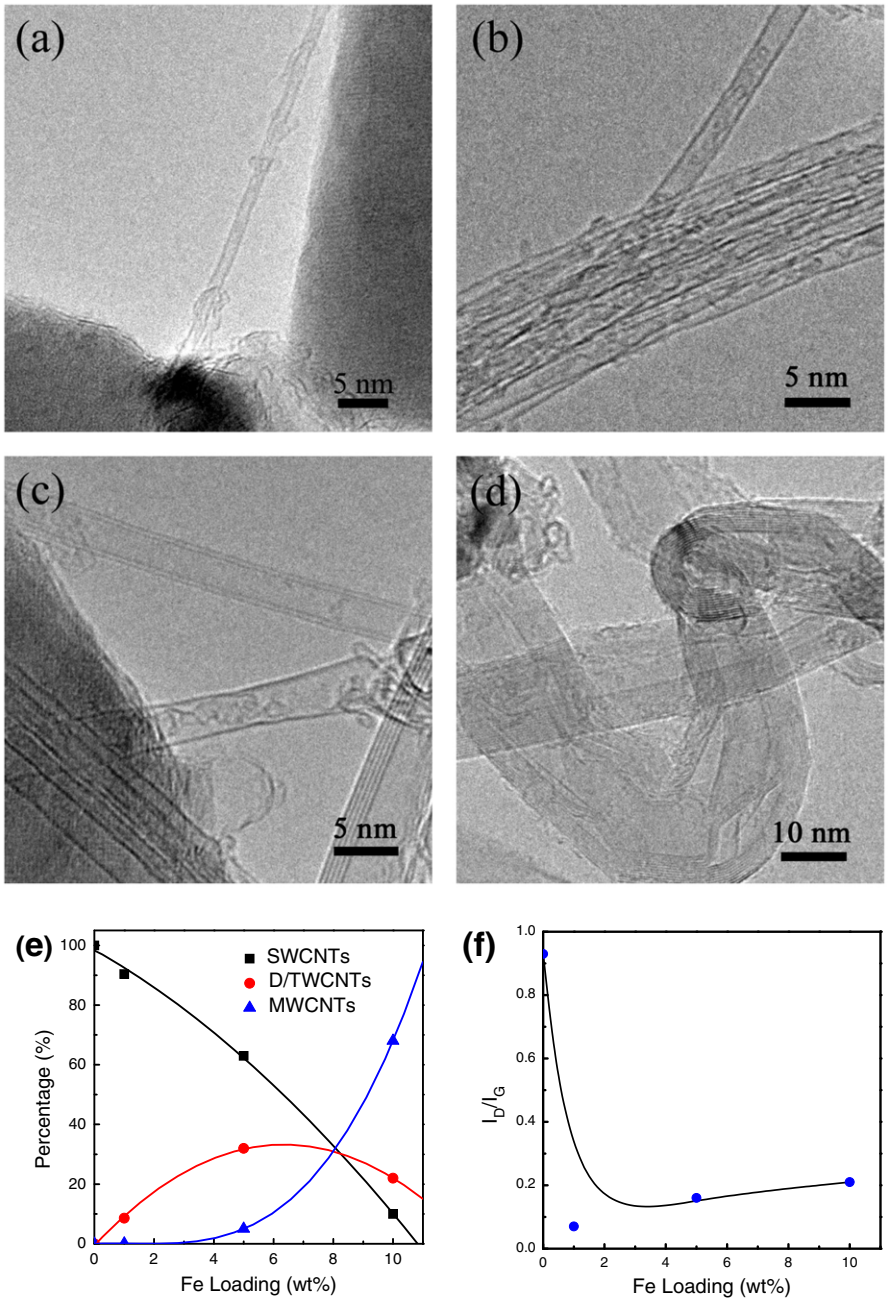

Fig. 5 – The structure of the CNTs formed on Fe-based catalysts with different loading amount at 900 °C for 15 min. The mass percentages of Fe on the sepiolite were (a) 0 wt.%, (b) 1 wt.%, (c) 5 wt.%, and (d) 10 wt.%. The comparison between the products obtained by catalysts A–D: (e) CNT type and (f) the ratio of I_D to I_G.

m^3. Based on the density and size distribution, the sepiolite agglomerates can be considered as Type A particles with good fluidization behavior according to Geldart particle classification. The fluidization characteristics of the sepiolite catalysts were investigated and the suitable gas velocity was defined to be 20 cm/s. Under this gas velocity, stable fluidization state can be achieved. CH_4 was introduced into the fluidized bed once the temperature reached 900 °C without reduction. The typical CNTs on the sepiolite were shown in Fig. 8. It can be found that small pieces of the sepiolite fibers inclined to gather into the large agglomerate after the reaction due to the entanglements of CNT bundles, which was indicated by the white arrows in Fig. 8a. High resolution TEM image of the products (Fig. 8b) illuminated that the CNTs in the fluidized bed reactor were mainly SWCNTs. The intensity ratio of the D to G band in the Raman spectra was 0.11, close to that in the fixed bed reactor. The yield of SWCNTs grown in fluidized bed was *ca.* 0.08 $g_{SWCNT}/g_{catalyst}$. The BET surface area of SWCNTs/cal-sepiolite was 61.61 m^2/g, and the BET surface area of SWCNTs was estimated to be 600 m^2/g.

The purity and yield of SWCNTs synthesized on sepiolites and other typical powder catalysts were listed in Table 3.

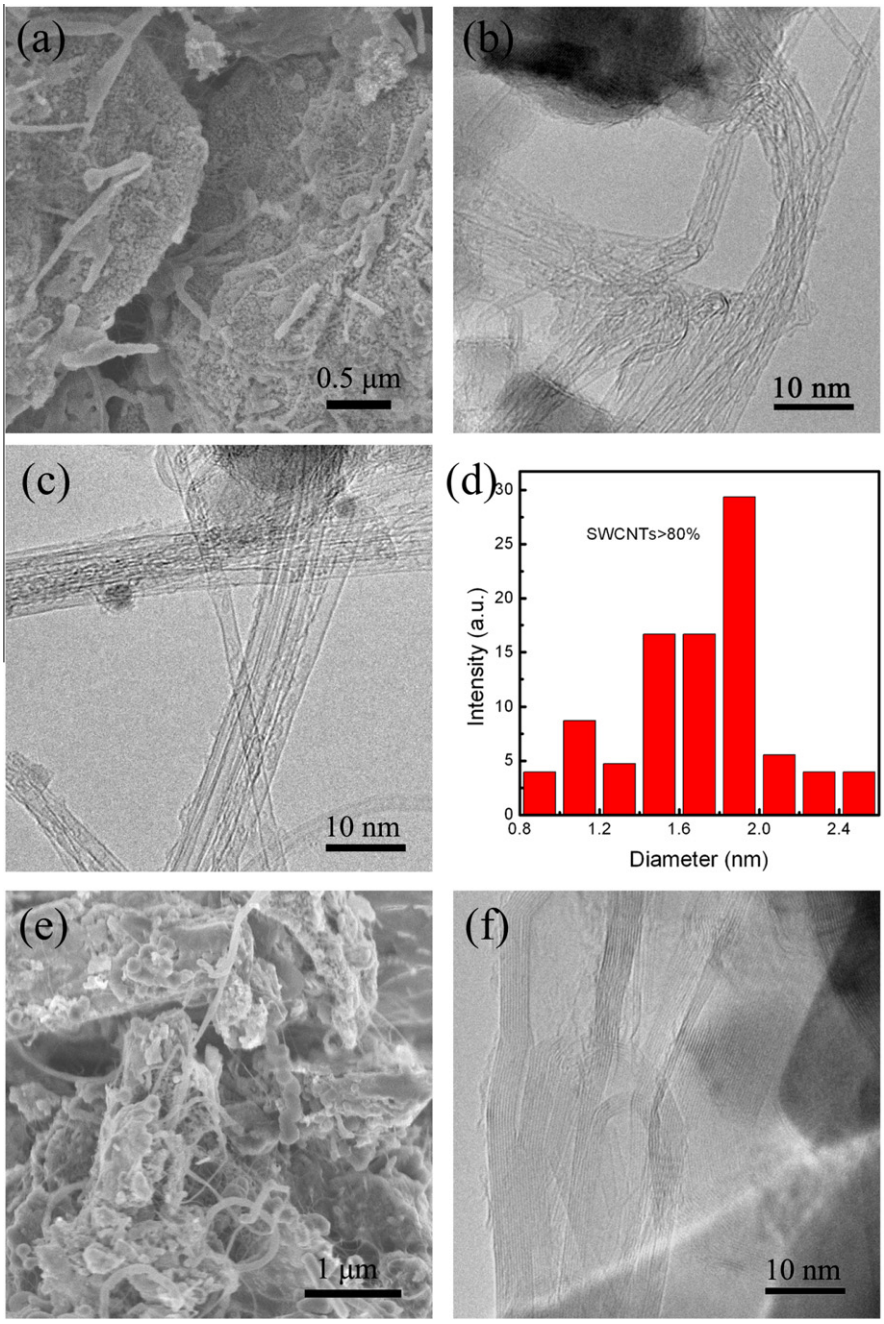

Fig. 6 – (a) SEM and (b) TEM images of the as-grown SWCNT sample on 1 wt.% Co/Mo/sepiolite catalyst (Co:Mo = 10:1). (c) TEM image and (d) the diameter distribution of the as-grown SWCNT sample on 5 wt.% Co/Mo/sepiolite catalyst (Co:Mo = 10:1). (e) SEM image and (f) TEM image of the as-grown SWCNT sample on 5 wt.% Co/Mo/sepiolite catalyst (Co:Mo = 3:1).

Firstly, the sepiolite was an efficient catalyst support for SWCNT growth both in a fixed bed and a fluidized bed. Secondly, the purity of SWCNT was competitive to those grown on well defined catalysts (such as Co/Mo/SiO_2, Fe/MgO, and Ni/Mg/Al LDHs). However, the yield of SWCNTs is not very high (Table 3). Natural materials always possess a complex composition, and some elements (such as K, P) were harmful for the high yield growth of CNTs. However, growth of SWCNTs on natural materials was a good solution towards diminishing our current dependence on nonrenewable feedstock for large-scale production of CNTs. Exploring an efficient way to synthesize high-quality SWCNTs with a high yield on natural materials is still highly interested.

3.6. *Adsorption of phenol with SWCNT/cal-sepiolite composite*

The performance of SWCNTs/cal-sepiolite in the adsorption of phenol was also investigated and the results were shown in Table 4 and Fig. 9. The two-parameter isotherm Langmuir

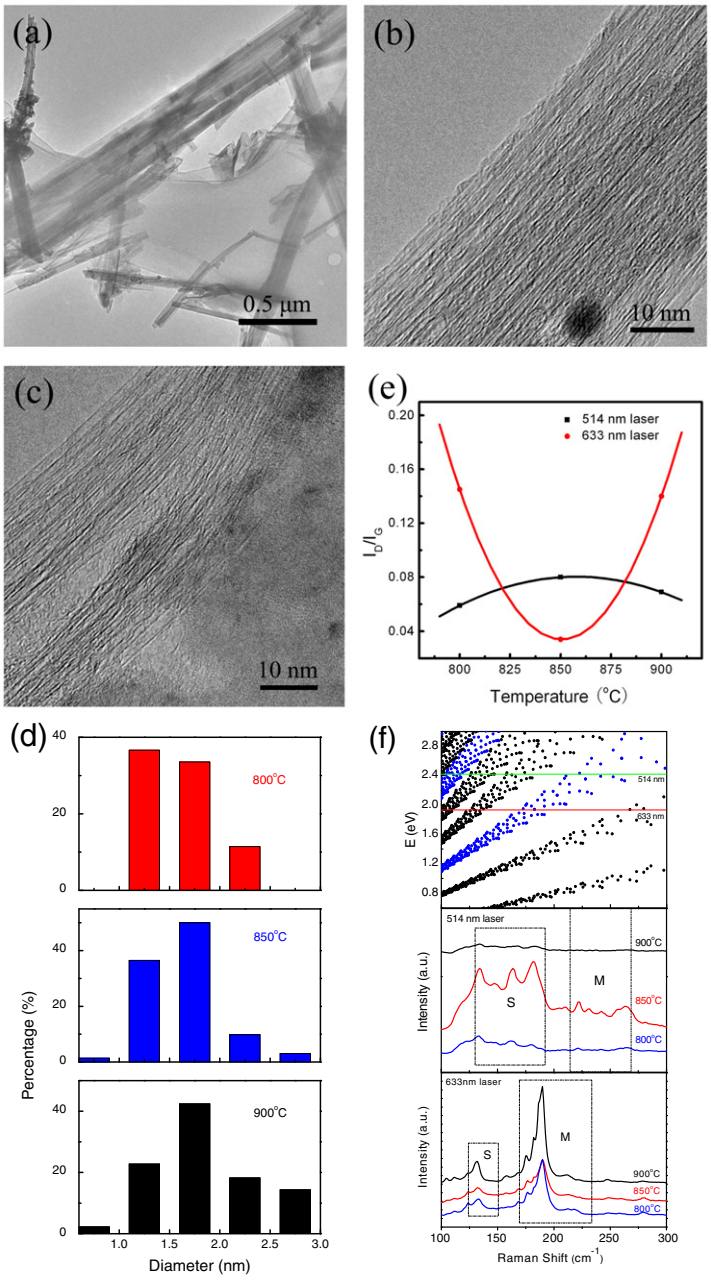

Fig. 7 – The TEM images of the SWCNTs grown among Fe/sepiolite catalyst for 15 min at (a) 750 °C, (b) 800 °C, and (c) 850 °C, respectively. (d) The diameter distributions of SWCNTs obtained at different temperatures. (e) The ratio of I_D/I_G and (f) the RBM patterns in the Raman spectra at excitation wavelength 633 and 514 nm for the as-grown SWCNT samples at different temperature.

equation was applied for further analysis of the adsorption data, expressed as [45],

$$Q_e = Q_L K_L C_e/(1 + K_L C_e) \quad (1)$$

where Q_e (mg/g) and C_e (mg/L) are equilibrium concentrations of phenol on the adsorbent and in the aqueous solution, respectively; Q_L is the monolayer adsorption capacity and K_L is the Langmuir constant.

The adsorptions on two adsorbents were highly nonlinear and the equilibrium data can fit the Langmuir model well, indicating that the adsorptions on two adsorbents were both monolayer type. The correlative parameters and the coefficient of determination r^2 were shown in Table 4. The Q_L value of the SWCNT/cal-sepiolite product was almost 12 times higher than that of natural sepiolite. The equilibrium adsorption amount was increased by ca. 10 times. In general, the BET surface area was recognized as a crucial factor affecting the adsorption capacity. The surface area varied disproportionally with the adsorption capacity. The adsorption isotherm per unit surface area was illuminated in Fig. 9, which described the similar trends per unit mass. The SWCNTs/cal-sepiolite illustrated strong adsorption abil-

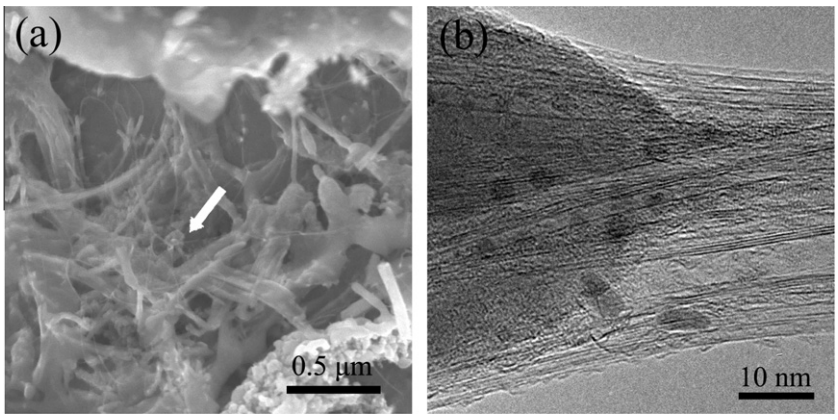

Fig. 8 – (a) SEM and (b) high resolution TEM images of SWCNT sample grown in a fluidized bed reactor at 900 °C.

Table 3 – Comparison of the SWCNTs grown on sepiolite and other catalyst supports.

Catalyst	Reactor[a]	Product	Purity[b]	Yield ($g_{SWCNT}/g_{catalyst}$)	Ref.
B	FxB	SWCNTs	90%	0.06	This work
B	FB	SWCNTs	80%	0.08	
F	FxB	S/DWCNTs	80%	–	
Co/Mo/SiO_2	FxB	SWCNTs	25–96%	0.33–2.2%	[42]
Ni/SiO_2	FB	SWCNTs	–	0.14	[43]
Fe/Mg/Al-LDH	FB	S/DWCNTs	54%	0.95	[44]
Ni/Mg/Al-LDH	FB	S/DWCNT	98%	0.17	
Fe/MgO	FxB	SWCNTs	–	0.05	[29]

[a] FB: fluidized bed; FxB: fixed bed.
[b] Purity: SWCNTs in the carbon products.

Table 4 – Langmuir model coefficients (Q_L and K_L) obtained from phenol adsorption at 30 °C.

Adsorbent	Q_L (mg/g)	K_L (L/mg)	r^2
SWCNTs/cal-sepiolite	155.8	0.0012	0.9989
Natural sepiolite	12.7	0.0016	0.9874

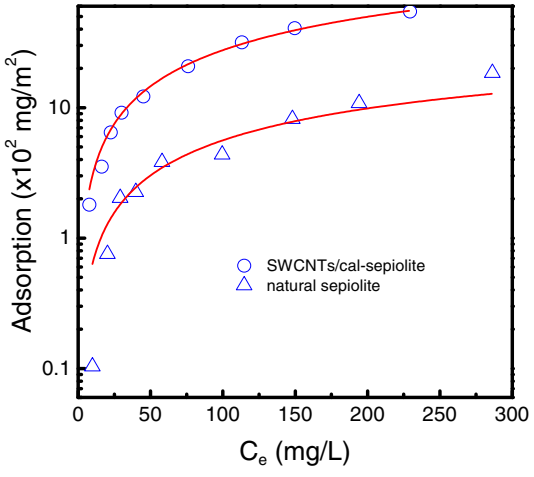

Fig. 9 – Adsorption isotherm of phenol on SWCNTs/cal-sepiolite and natural sepiolite at 30 °C, in which the hollow symbols were experimental data and the solid lines are Langmuir model.

ity of phenol, whose result can be inferred from the fact that π–π electron-donor–acceptor (EDA) interactions enhance the adsorption of phenol (π-electron acceptors) due to π-electron-rich regions (π-electron donors) on the SWCNT surface [27]. Thus, it should be pointed out that the SWCNT/cal-sepiolite product was a good composite for the adsorption of phenol on adsorption capacity per unit mass and per unit surface area.

4. Conclusion

High-quality SWCNTs with large aspect ratio were efficiently synthesized on low-cost sepiolite mineral which was pretreated through an ion-exchange route. The structure of the CNTs was further modified by controlling the catalyst composition and changing the growth conditions. An Fe-based catalyst at low loading amount (1 wt.%) showed excellent activity for the growth of SWCNTs, while the Co/Mo-based catalyst showed higher selectivity to small diameter SWCNTs. The chirality and diameter distribution were highly depended on the reaction temperature. The synthesis of SWCNTs can also be scaled up in a fluidized bed reactor for mass production. Finally, the as-grown SWCNT/cal-sepiolite product was demonstrated to be one kind of advanced functional materials for the adsorption of phenol with an adsorption capacity of 155.8 mg/g. This provides an interesting route to transfer natural materials into advanced materials with potential applications for environmental protection.

Acknowledgements

The work was supported by the Foundation for the Natural Scientific Foundation of China (No. 20736004, No. 20736007, No. 2007AA03Z346), the China National Program (No. 2006CB0N0702).

REFERENCES

[1] Zhou WY, Bai XD, Wang EG, Xie SS. Synthesis, structure, and properties of single-walled carbon nanotubes. Adv Mater 2009;21(45):4565–83.
[2] Padture NP. Multifunctional composites of ceramics and single-walled carbon nanotubes. Adv Mater 2009;21(17):1767–70.
[3] Kawasaki S, Iwai Y, Hirose M. Electrochemical lithium ion storage properties of single-walled carbon nanotubes containing organic molecules. Carbon 2009;47(4):1081–6.
[4] Kim YA, Kojima M, Muramatsu H, Umemoto S, Watanabe T, Yoshida K, et al. In situ Raman study on single- and double-walled carbon nanotubes as a function of lithium insertion. Small 2006;2(5):667–76.
[5] Liu ZF, Jiao LY, Yao YG, Xian XJ, Zhang J. Aligned, ultralong single-walled carbon nanotubes: From synthesis, sorting, to electronic devices. Adv Mater 2010;22(21):2285–310.
[6] Su DS. The use of natural materials in nanocarbon synthesis. ChemSusChem 2009;2(11):1009–20.
[7] Su DS, Chen XW. Natural lavas as catalysts for efficient production of carbon nanotubes and nanofibers. Angew Chem Int Ed 2007;46(11):1823–4.
[8] Su DS, Chen XW, Liu X, Delgado JJ, Schlogl R, Gajovic A. Mount-Etna-Lava-supported nanocarbons for oxidative dehydrogenation reactions. Adv Mater 2008;20(19):3597–600.
[9] Endo M, Takeuchi K, Kim YA, Park KC, Ichiki T, Hayashi T, et al. Simple synthesis of multiwalled carbon nanotubes from natural resources. ChemSusChem 2008;1(10):820–2.
[10] Zhao MQ, Zhang Q, Huang JQ, Nie JQ, Wei F. Advanced materials from natural materials: synthesis of aligned carbon nanotubes on wollastonites. ChemSusChem 2010;3(4):453–9.
[11] Rinaldi A, Zhang J, Mizera J, Girgsdies F, Wang N, Hamid SBA, et al. Facile synthesis of carbon nanotube/natural bentonite composites as a stable catalyst for styrene synthesis. Chem Commun 2008;(48):6528–6530.
[12] Kawasaki S, Shinoda M, Shimada T, Okino F, Touhara H. Single-walled carbon nanotubes grown on natural minerals. Carbon 2006;44(11):2139–41.
[13] Gournis D, Karakassides MA, Bakas T, Boukos N, Petridis D. Catalytic synthesis of carbon nanotubes on clay minerals. Carbon 2002;40(14):2641–6.
[14] Zhang WD, Phang IY, Liu TX. Growth of carbon nanotubes on clay: Unique nanostructured filler for high-performance polymer nanocomposites. Adv Mater 2006;18(1):73–7.
[15] Zhang Q, Zhao MQ, Liu Y, Cao AY, Qian WZ, Lu YF, et al. Energy-absorbing hybrid composites based on alternate carbon-nanotube and inorganic layers. Adv Mater 2009;21(28):2876–80.
[16] Zhang Q, Zhao MQ, Huang JQ, Liu Y, Wang Y, Qian WZ, et al. Vertically aligned carbon nanotube arrays grown on a lamellar catalyst by fluidized bed catalytic chemical vapor deposition. Carbon 2009;47(11):2600–10.
[17] Zhang Q, Zhao MQ, Huang JQ, Nie JQ, Wei F. Mass production of aligned carbon nanotube arrays grown on clay by fluidized bed catalytic chemical vapor deposition. Carbon 2010;48(4):1196–209.
[18] Su DS, Chen XW, Weinberg G, Klein-Hofmann A, Timpe O, Hamid SBA, et al. Hierarchically structured carbon: synthesis of carbon nanofibers nested inside or immobilized onto modified activated carbon. Angew Chem Int Ed 2005;44(34):5488–92.
[19] Chen XW, Timpe O, Hamid SBA, Schlogl R, Su DS. Direct synthesis of carbon nanofibers on modified biomass-derived activated carbon. Carbon 2009;47(1):340–3.
[20] Rinaldi A, Abdullah N, Ali M, Furche A, Hamid SBA, Su DS, et al. Controlling the yield and structure of carbon nanofibers grown on a nickel/activated carbon catalyst. Carbon 2009;47(13):3023–33.
[21] Dunens OM, MacKenzie KJ, Harris AT. Synthesis of multi-walled carbon nanotubes on 'red mud' catalysts. Carbon 2010;48(8):2375–7.
[22] Darder M, Lopez-Blanco M, Aranda P, Aznar AJ, Bravo J, Ruiz-Hitzky E. Microfibrous chitosan-sepiolite nanocomposites. Chem Mater 2006;18(6):1602–10.
[23] Aranda P, Kun R, Martin-Luengo MA, Letaief S, Dekany I, Ruiz-Hitzky E. Titania-Sepiolite nanocomposites prepared by a surfactant templating colloidal route. Chem Mater 2008;20(1):84–91.
[24] Kuang WX, Facey GA, Detellier C, Casal B, Serratosa JM, Ruiz-Hitzky E. Nanostructured hybrid materials formed by sequestration of pyridine molecules in the tunnels of sepiolite. Chem Mater 2003;15(26):4956–67.
[25] Gomez-Aviles A, Darder M, Aranda P, Ruiz-Hitzky E. Multifunctional materials based on graphene-like/sepiolite nanocomposites. Appl Clay Sci 2010;47(3–4):203–11.
[26] Fernandez-Saavedra R, Aranda P, Ruiz-Hitzky E. Templated synthesis of carbon nanofibers from polyacrylonitrile using sepiolite. Adv Funct Mater 2004;14(1):77–82.
[27] Chen JY, Chen W, Zhu D. Adsorption of nonionic aromatic compounds to single-walled carbon nanotubes: effects of aqueous solution chemistry. Environ Sci Technol 2008;42(19):7225–30.
[28] Sandi G, Winans RE, Seifert S, Carrado KA. In situ SAXS studies of the structural changes of sepiolite clay and sepiolite-carbon composites with temperature. Chem Mater 2002;14(2):739–42.
[29] Nie JQ, Qian WZ, Zhang Q, Wen Q, Wei F. Very high-quality single-walled carbon nanotubes grown using a structured and tunable porous Fe/MgO catalyst. J Phys Chem C 2009;113(47):20178–83.
[30] Lim S, Li N, Fang F, Pinault M, Zoican C, Wang C, et al. High-yield single-walled carbon nanotubes synthesized on the small-pore (C10) Co-MCM-41 catalyst. J Phys Chem C 2008;112(32):12442–54.
[31] Hiraoka T, Kawakubo T, Kimura J, Taniguchi R, Okamoto A, Okazaki T, et al. Selective synthesis of double-wall carbon nanotubes by CCVD of acetylene using zeolite supports. Chem Phys Lett 2003;382(5–6):679–85.
[32] Kobayashi K, Kitaura R, Kumai Y, Goto Y, Inagaki S, Shinohara H. Fabrication of single-wall carbon nanotubes within the channels of a mesoporous material by catalyst-supported chemical vapor deposition. Carbon 2009;47(3):722–30.
[33] Dresselhaus MS, Dresselhaus G, Saito R, Jorio A. Raman spectroscopy of carbon nanotubes. Phys Rep 2005;409(2):47–99.
[34] Nasibulin AG, Pikhitsa PV, Jiang H, Kauppinen EI. Correlation between catalyst particle and single-walled carbon nanotube diameters. Carbon 2005;43(11):2251–7.
[35] Harutyunyan AR, Tokune T, Mora E, Yoo JW, Epstein AJ. Evolution of catalyst particle size during carbon single walled nanotube growth and its effect on the tube characteristics. J Appl Phys 2006;100(4):044321-1-8.
[36] Zhang Q, Huang JQ, Zhao MQ, Qian WZ, Wei F. Modulating the diameter of carbon nanotubes in array form via floating

catalyst chemical vapor deposition. Appl Phys A 2009;94(4):853–60.
[37] Li XL, Tu XM, Zaric S, Welsher K, Seo WS, Zhao W, et al. Selective synthesis combined with chemical separation of single-walled carbon nanotubes for chirality selection. J Am Chem Soc 2007;129(51):15770–1.
[38] Irurzun VM, Tan YQ, Resasco DE. Sol–Gel synthesis and characterization of Co-Mo/silica catalysts for single-walled carbon nanotube production. Chem Mater 2009;21(11):2238–46.
[39] Li N, Wang XM, Ren F, Haller GL, Pfefferle LD. Diameter tuning of single-walled carbon nanotubes with reaction temperature using a Co monometallic catalyst. J Phys Chem C 2009;113(23):10070–8.
[40] Okamoto A, Shinohara H. Control of diameter distribution of single-walled carbon nanotubes using the zeolite-CCVD method at atmospheric pressure. Carbon 2005;43(2):431–6.
[41] Kataura H, Kumazawa Y, Maniwa Y, Umezu I, Suzuki S, Ohtsuka Y, et al. Optical properties of single-wall carbon nanotubes. Synthetic Met 1999;103(1–3):2555–8.
[42] Alvarez WE, Kitiyanan B, Borgna A, Resasco DE. Synergism of Co and Mo in the catalytic production of single-wall carbon nanotubes by decomposition of CO. Carbon 2001;39(4):547–58.
[43] Li YL, Kinloch IA, Shaffer MS, Geng JF, Johnson B, Windle AH. Synthesis of single-walled carbon nanotubes by a fluidized-bed method. Chem Phys Lett 2004;384(1–3):98–102.
[44] Zhao MQ, Zhang Q, Huang JQ, Nie JQ, Wei F. Layered double hydroxides as catalysts for the efficient growth of high quality single-walled carbon nanotubes in a fluidized bed reactor. Carbon 2010;48(11):3260–70.
[45] Li YH, Ding J, Luan ZK, Di ZC, Zhu YF, Xu CL, et al. Competitive adsorption of Pb^{2+}, Cu^{2+} and Cd^{2+} ions from aqueous solutions by multiwalled carbon nanotubes. Carbon 2003;41(14):2787–92.